Defect-induced magnetic order in pure ZnO films

M. Khalid,[1] M. Ziese,[1] A. Setzer,[1] P. Esquinazi,[1] M. Lorenz,[2] H. Hochmuth,[2] M. Grundmann,[2] D. Spemann,[3] T. Butz,[3] G. Brauer,[4] W. Anwand,[4] G. Fischer,[5] W. A. Adeagbo,[5] W. Hergert,[5] and A. Ernst[6]

[1]*Division of Superconductivity and Magnetism, University of Leipzig, 04103 Leipzig, Germany*

[2]*Semiconductor Physics Group, University of Leipzig, 04103 Leipzig, Germany*

[3]*Division of Nuclear Solid State Physics, University of Leipzig, 04103 Leipzig, Germany*

[4]*Institut für Ionenstrahlphysik und Materialforschung, Forschungszentrum Dresden-Rossendorf, 01314 Dresden, Germany*

[5]*Institute of Physics, Martin Luther University Halle–Wittenberg, Von-Seckendorff-Platz 1, 06120 Halle, Germany*

[6]*Max Planck Institute of Microstructure Physics, Weinberg 2, 06120 Halle, Germany*

(Received 20 May 2009; revised manuscript received 23 June 2009; published 30 July 2009)

We have investigated the magnetic properties of pure ZnO thin films grown under N_2 pressure on *a*-, *c*-, and *r*-plane Al_2O_3 substrates by pulsed-laser deposition. The substrate temperature and the N_2 pressure were varied from room temperature to 570 °C and from 0.007 to 1.0 mbar, respectively. The magnetic properties of bare substrates and ZnO films were investigated by SQUID magnetometry. ZnO films grown on *c*- and *a*-plane Al_2O_3 substrates did not show significant ferromagnetism. However, ZnO films grown on *r*-plane Al_2O_3 showed reproducible ferromagnetism at 300 K when grown at 300–400 °C and 0.1–1.0 mbar N_2 pressure. Positron annihilation spectroscopy measurements as well as density-functional theory calculations suggest that the ferromagnetism in ZnO films is related to Zn vacancies.

DOI: 10.1103/PhysRevB.80.035331 PACS number(s): 75.50.Pp, 75.70.−i

I. INTRODUCTION

After the theoretical prediction of room temperature ferromagnetism in Mn-doped ZnO,[1] ZnO doped with magnetic transition metal ions was intensively studied due to its potential electronic applications. Among these metal ions Co-doped ZnO was thought to lead to an intrinsic, homogeneous semiconducting ferromagnet. However, x-ray magnetic circular dichroism measurements on the magnetic Co-ZnO films revealed that none of the elements behave ferromagnetically and consequently the observed ferromagnetism was attributed to O or Zn vacancies.[2,3] Room temperature ferromagnetism has also been observed in undoped wide-band gap semiconducting thin films and nanoparticles such as, e.g., TiO_2, HfO_2, In_2O_3, and CeO_2.[4–6] The observation of ferromagnetism in these undoped systems opened a wide debate on its origin. As in graphite—the paradigma for defect-induced magnetism—vacancies as well as nonmagnetic adatoms such as H may play a role in the observed magnetic order.[7] Recently, ferromagnetism was found in a single ZnO film grown on a-plane Al_2O_3 under N_2 pressure but without demonstrating its reproducibility.[8] To our knowledge, there is no report on a systematic study of the magnetic properties of pure ZnO films grown under N_2 pressure. The aim of this communication is to show that reproducible room temperature ferromagnetism can be induced in pulsed laser deposited (PLD) pure ZnO films under N_2 pressure at certain growth conditions.

II. EXPERIMENTAL DETAILS

ZnO films were grown from a ZnO polycrystalline target on 6×6 mm^2 *a*-, *c*-, and *r*-plane Al_2O_3 substrates by PLD under N_2 pressure using a KrF excimer laser. The purity of the ZnO powder used for the preparation of the PLD target was 5N. In order to reduce the iron contamination of the ZnO films as much as possible in the given PLD chamber, a specially designed molybdenium substrate holder was used for film growth. Three sets of ZnO films (films on *a*-, *b*- and *c*-plane sapphire substrates) were grown at different substrate temperatures and N_2 pressures. The film thickness was between 60–400 nm. The film thickness was controlled by the number of laser pulses with a fluence of 2 J cm^{-2}. We performed Rutherford backscattering spectroscopy (RBS) and particle induced x-ray emission (PIXE) measurements to estimate and analyze the thickness and the composition of films, respectively. The crystal structure was characterized by x-ray diffraction (XRD) θ-2θ scans using a CuK_α source. The magnetic properties were determined by SQUID (superconducting quantum interface device) magnetometry. For each ZnO film, a hysteresis loop was measured at 5 and 300 K as well as temperature dependent measurements of the magnetic moment (MM) and its remanence were investigated. We have used nonmagnetic tweezers and the sample was directly mounted in a straw to avoid magnetic background signals. Positron annihilation spectroscopy (PAS) was used to investigate the variation of the vacancy concentration with N_2 pressure given by the Doppler broadening parameter S.[9,10]

III. RESULTS AND DISCUSSIONS

To elucidate experimental results, first-principle calculations were performed based on density-functional theory in the generalized gradient approximation (GGA).[11–13] Electronic correlations were accounted within a GGA+*U* approximation. The calculations were carried out with the Vienna *ab initio* simulation package[14,15] using the projector augmented-wave method.[16] Defects in ZnO were simulated with a $2(3)\times2\times2$ supercells containing 64 (96) atoms built from a conventional orthorhombic unit cell of 8 atoms. The expansion of the electronic wave functions in plane waves

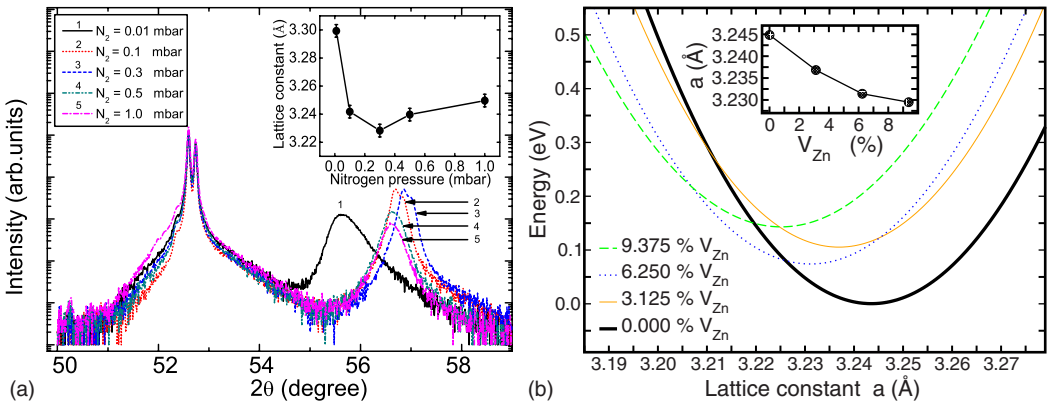

FIG. 1. (Color online) (a) XRD pattern of ZnO films grown on *r*-plane sapphire substrates at five different nitrogen pressures. The inset shows the variation of the lattice parameter a of ZnO films with N_2 partial pressure (film thickness: 500, 400, 430, 65, and 60 nm grown on 0.01 mbar, 0.1 mbar, 0.3 mbar, 0.5, and 1.0 mbar N_2 pressure, respectively). (b) First-principles results showing a left shift in the minima of energy-lattice curves indicating a decrease in the lattice constants with respect to the increase in Zn vacancy V_{Zn} concentration (see inset). Here, one V_{Zn} in a 64 atoms supercell corresponds to a concentration of 3.125%. Due to the differences in the total energy E between the four calculated supercells E has been shifted by $7n$ eV, n being the number of vacancies per supercell, in order to allow direct comparison in one graph.

was done using the cut-off energy of 400 eV with a Monkhorst Pack k-points mesh of $3(2)\times2\times2$. The calculated lattice constants of $a=3.245$ Å and the c/a ratio of 1.603 were comparable to the experimental values (3.249 Å and 1.602, respectively[17]) when we applied the on-site Coulomb correlation energy correction $U=5.7$ eV. The band gap obtained with this parameter is of order of the 1.3 eV.

Figure 1(a) shows the XRD patterns of ZnO films grown on *r*-plane sapphire substrates at 400 °C substrate temperature and at 0.01–1.0 mbar N_2 pressure. The peak near $2\theta=56.6°$ is attributed to the ZnO (110) reflection. The XRD patterns indicate that there is an epitaxial relationship of $ZnO(0002)\|Al_2O_3(11\bar{2}0)$, $ZnO(0002)\|Al_2O_3(0001)$, and $ZnO(11\bar{2}0)\|Al_2O_3(01\bar{1}2)$ for films grown on *a*-, *c*-, and *r*-plane Al_2O_3 substrates, respectively. The lattice constant a and its change with N_2 pressure was calculated from the location of the $(11\bar{2}0)$ reflection peak, see inset to Fig. 1(a). A decrease of the lattice constant a is observed with increasing N_2 pressure at the growth temperature of 400 °C.

This experimental finding was confirmed by our first-principles investigations. Theoretical calculations, presented in Fig. 1(b), show that an increase in the concentration of Zn vacancies (V_{Zn}) leads to an effective reduction of the equilibrium lattice constant a. The reduction of lattice constant a obtained for O vacancies (V_o) for the same concentration as V_{Zn} is only about one third of the one observed for Zn vacancies. No significant volume change occurs if a Zn or O atom is replaced by N. This strongly suggests the formation of Zn vacancies, which induce a high magnetic moment $MM\simeq2\mu_B$ distributed over the neighboring O atoms. Also, our calculations indicate that in case O or Zn are replaced by N the formed localized MM's are smaller. Interestingly, our results show that H atoms neither improve the formation of MM's at defects nor form isolated magnetic defects by themselves.[18]

The inset to Fig. 1(a) shows a gradual increase of lattice constant a at higher N_2 pressure (0.5–1.0 mbar). This increase in lattice constant a at higher N_2 pressure might be due to the strain. However, we leave this question open for future work.

The saturation magnetization of ZnO films grown on *a*-, *c*- and *r*-plane sapphire substrates is shown in Fig. 2(a). ZnO films grown on *a*- and *c*-plane sapphire substrates at several temperatures and nitrogen pressures ranging from room temperature to 570 °C and from 0.007 to 1.0 mbar did not show significant ferromagnetic contributions in contrast to the re-

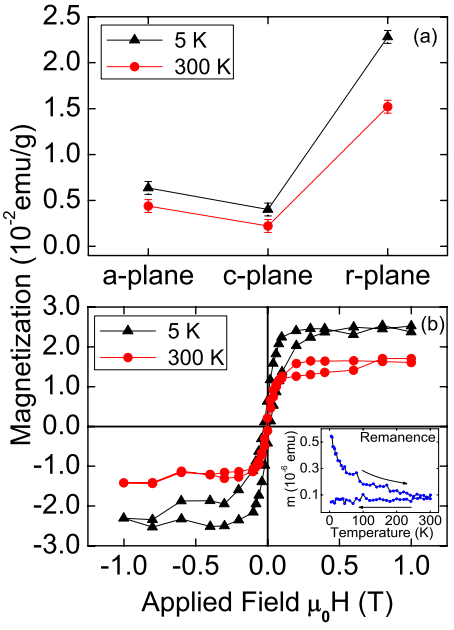

FIG. 2. (Color online) (a) The saturation magnetization of ZnO films grown on *a*-, *c*-, and *r*-plane sapphire substrates measured at 5 and 300 K. (b) Hysteresis loops of a ZnO film (after the subtraction of background signals, 0.3 mbar N_2 pressure, 430 nm thick film) grown on a *r*-plane sapphire substrate measured at 5 and 300 K by using SQUID magnetometry with a field of 1 T parallel to the film planes. The inset shows the remanence of the same sample.

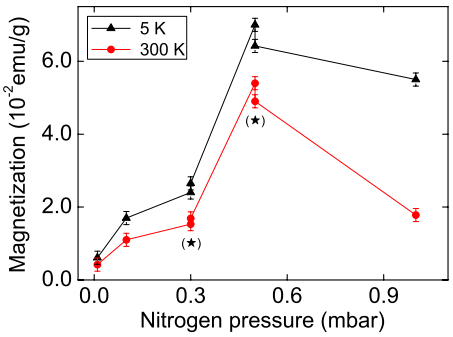

FIG. 3. (Color online) The saturation magnetization of ZnO films grown at 400 °C on *r*-plane sapphire vs N_2 partial pressure at 5 and 300 K. The points marked with (★) are from four independently prepared samples. Two samples were grown at 0.3 mbar N_2 pressure while other two samples were grown at 0.5 mbar N_2 pressure keeping the substrate temperature constant, i.e., 400 °C. Each data point correspond to the magnetization of a single ZnO film. The thickness of ZnO films was between 60–500 nm. The error bars in the figure are $\lesssim$15%.

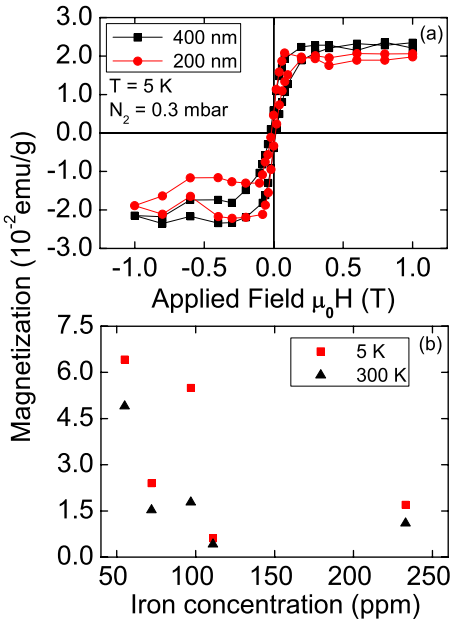

FIG. 4. (Color online) (a) The magnetization of ZnO films with different thicknesses vs. the applied magnetic field measured at 5 K (The slight lack of symmetry in the Hysteresis loop is due to SQUID resolution, i.e., extraction of ferromagnetic contribution from large diamagnetic signals). (b) The saturation magnetization of ZnO films vs iron concentration of ZnO films. This figure demonstrates clearly that there is no correlation between the iron concentration and the magnetization of the ZnO films.

sults of Ref. 8. We note that it is difficult to control the electrical and the magnetic properties of ZnO films grown on *a*-plane sapphire due to the polarity of their O- or Zn-terminated surfaces. On the other hand ZnO films grown on *r*-plane sapphire substrates are nonpolar and are composed of both Zn and O atoms. It appears easier for defects such as O vacancies, Zn interstitials and vacancies to form during the film growth.[19] This might be one of the reasons why reproducible ferromagnetism arises only for ZnO films grown on *r*-plane sapphire substrates as we describe below.

Figure 2(b) shows the magnetization of a ZnO film measured at 5 and 300 K. A clear ferromagnetic hysteresis loop is observed at 300 K. The difference between saturation magnetization M_s at 5 and 300 K suggests a Curie temperature clearly above 300 K. The inset in Fig. 2(b) shows the irreversible behavior of the remnant MM for the same ZnO film. Its irreversible behavior vs. temperature is the typical one for ferromagnets. Figure 3 shows the saturation magnetization of ZnO films grown under different N_2 pressures at a constant substrate temperature of 400 °C. The magnetization of ZnO films increases with N_2 pressure tending to a maximum at 0.5 mbar. This saturation effect can be understood by looking once more at our theoretical calculations. They show that defects that carry a magnetic moment when isolated can become nonmagnetic when coming close to other defects or forming pairs. For example, if V_{Zn} (MM$\simeq 2\mu_B$) and V_O (MM=0) are brought close together, i.e., are present in one supercell of 96 atoms, the MM around V_{Zn} vanishes. An increase in concentration has the effect of reducing the mean distance between defects. Therefore, growing more defects into an already ferromagnetic sample increases the probability of creating magnetically annihilating defects near already existing magnetic and ferromagnetically coupled defects. Since a growing N_2 pressure is assumed to increase the defect concentration, it follows that there is a pressure beyond which the magnetization of the sample does not grow any further or may even be reduced. The maximum value of saturation magnetization of ZnO films at 300 K was 0.05 emu/g, about two orders of magnitude higher than those reported in the literature.[4–6,8,20]

We note that the calculated magnetization values are a lower limit; the (certainly smaller) ferromagnetic mass in the samples remains unknown. It is rather evident that the induced magnetic state cannot be homogeneous but should consist of patches with the appropriate defect density. In agreement with this interpretation our calculations indicate that the magnetization is much larger for a defect concentration that allows for percolation of the magnetic interaction, e.g., for 5% V_{Zn} $M \simeq 7$ emu/g.

ZnO films grown under N_2 pressure can suffer highly tensile strain due to the lattice mismatch and the difference of the coefficients of thermal expansion of ZnO and Al_2O_3. Therefore, it is appropriate to investigate whether the observed ferromagnetism arises from the interface between substrate and film as reported in Refs. 21 and 22. We have grown few ZnO films varying the film thickness at similar growth conditions. Reducing the film thickness to one half the MM also decreases by a similar factor (the magnetization scales to the mass of ZnO films) see Fig. 4(a) indicating that the observed ferromagnetism in ZnO films is not due to an interface effect.

Figure 4(b) shows the magnetization at saturation vs Fe concentration observed for all our samples. We note that 50 ppm Fe, if ferromagnetic, would give a magnetic moment of 1×10^{-7} emu in a 100 nm thick film, representing a magnetization of V_{Zn} emu/g, i.e., the value one order of magnitude smaller than observed one. From the data of Fig. 4(b), we conclude that the Fe did not influence the ferromagnetic

properties of ZnO films in agreement with other reports.[21,23] The influence of other impurities as Ti(30 ppm) and Cr(10 ppm) can also be ruled out.

Positron annihilation spectroscopy (PAS) can be used to analyze vacancy-type defects in ZnO films. The measurements were carried out with the monoenergetic positron beam "SPONSOR" at Rossendorf[24] at which a variation of the positron energy E from 30 eV to 36 keV is possible. The energy resolution of the Ge detector at 511 keV is (1.09 ± 0.01) keV, resulting in a high sensitivity to changes in material properties from surface to depth. About 5×10^5 events per spectrum were accumulated. The motion of electron-positron pair prior to annihilation causes Doppler broadening of the 511 keV annihilation line and can be characterized by the line-shape parameter S. In brief, the value of S is defined by the ratio of counts in the central region of the annihilation gamma peak to the total number of counts in the peak. It is common to define the central region for a certain sample to obtain $S_{bulk} \sim 0.5$ for the ZnO reference sample. Then a S parameter higher than 0.5 refers to vacancy-type defects in the sample due to the more likely annihilation of positrons with low momentum electrons in this region. For a more general discussion of the parameter we refer to the literature.[25]

The Doppler broadening parameter S of ZnO films grown on r-plane sapphire at 400 °C under different N_2 pressure as a function of incident positron energy is shown in Fig. 5. Mainly three different annihilation regions are visible: Positrons with an energy below 2 keV annihilate at and near the surface of the sample. Between 2 and 6 keV the $S(E)$ curve mainly represents the annihilation within the grown ZnO layers. Finally, at energies higher than 6 keV the influence of the sapphire substrate becomes visible. The insert to Fig. 5 illustrates the dependence of the S parameter of the ZnO films on different N_2 partial pressure at a fixed positron energy. A strong increase of the S parameter at 0.5 mbar N_2 pressure was detected, which clearly indicates the presence of vacancy-type defects larger than in the ZnO layers grown with N_2 pressures below 0.5 mbar. The increase of the S parameter at 0.5 mbar correlates with the drastic increase of the saturation magnetization of ZnO films as shown in Fig. 3. Therefore, it is concluded that the creation of larger vacancy-type defects is related with the observed ferromagnetism in pure ZnO films in agreement with our theoretical results. However, the real size of these vacancy-type defects and their structure remain to be determined and a challenge for future work.

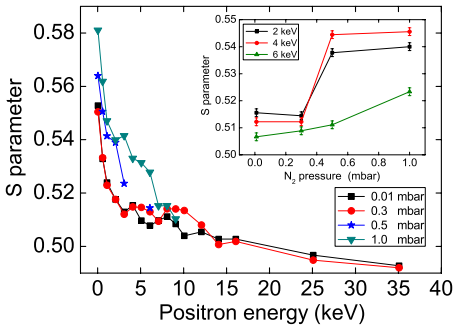

FIG. 5. (Color online) Doppler broadening parameter S (proportional to the vacancy concentration) vs incident positron energy E of ZnO films grown under different N_2 pressures at 400 °C substrate temperature. Inset shows the value of S parameter vs N_2 pressure at fixed positron energies.

IV. CONCLUSION

In conclusion, we have investigated the magnetic properties of ZnO films grown on a-, c-, and r-plane sapphire substrates under N_2 partial pressure. ZnO films grown only on r-plane sapphire substrates at 400 °C substrate temperature and 0.1–1.0 mbar N_2 pressure showed reproducible room temperature ferromagnetism. There is a correlation between the magnetization of ZnO films, the N_2 pressure and the vacancy concentration, which together with our theoretical calculations suggest that Zn vacancies are probably the reason for the defect induced magnetic order.

This work is supported by the Sonderforschungsbereich under Grant No. SFB 762, "Functionality of Oxide Interfaces." The calculations were performed at the John von Neumann Institute in Jülich and Rechenzentrum Garching of the Max Planck Society (Germany).

[1] T. Dietl, H. Ohno, F. Matsukura, J. Cibert, and D. Ferrand, Science **287**, 1019 (2000).
[2] M. Gacic, G. Jakob, C. Herbort, H. Adrian, T. Tietze, S. Brück, and E. Goering, Phys. Rev. B **75**, 205206 (2007).
[3] Q. Wang, Q. Sun, G. Chen, Y. Kawazoe, and P. Jena, Phys. Rev. B **77**, 205411 (2008).
[4] M. Venkatesan, C. Fitzgerald, and J. Coey, Nature (London) **430**, 630 (2004).
[5] J. M. D. Coey, M. Venkatesan, P. Stamenov, C. B. Fitzgerald, and L. S. Dorneles, Phys. Rev. B **72**, 024450 (2005).
[6] N. H. Hong, N. Poirot, and J. Sakai, Appl. Phys. Lett. **89**, 042503 (2006).
[7] P. Esquinazi, *Handbook of Magnetism and Advanced Magnetic Materials* (John Wiley & Sohn Ltd, Chichester, UK, 2007), Vol. 4, pp. 2256–2281.
[8] Q. Xu, H. Schmidt, L. Hartmann, H. Hochmuth, M. Lorenz, A. Setzer, P. Esquinazi, C. Meinecke, and M. Grundmann, Appl. Phys. Lett. **91**, 092503 (2007).
[9] G. Brauer, W. Anwand, W. Skorupa, J. Kuriplach, O. Melikhova, C. Moisson, H. von Wenckstern, H. Schmidt, M. Lorenz, and M. Grundmann, Phys. Rev. B **74**, 045208 (2006).
[10] *Positron Spectroscopy of Solids, Proceedings of the International School of Physics, Varenna, 1993*, edited by A. Dupasquier and A. P. Mills, Jr. (IOS Press, Amsterdam, 1995).
[11] P. Hohenberg and W. Kohn, Phys. Rev. **136**, B864 (1964).
[12] W. Kohn and L. J. Sham, Phys. Rev. **140**, A1133 (1965).

[13] J. P. Perdew, J. A. Chevary, S. H. Vosko, K. A. Jackson, M. R. Pederson, D. J. Singh, and C. Fiolhais, Phys. Rev. B **46**, 6671 (1992).
[14] G. Kresse and J. Hafner, Phys. Rev. B **47**, 558 (1993).
[15] G. Kresse and J. Furthmüller, Comput. Mater. Sci. **6**, 15 (1996).
[16] P. E. Blöchl, Phys. Rev. B **50**, 17953 (1994).
[17] K. Yoshio, A. Onodera, H. Satoh, N. Sakagami, and H. Yamashita, Ferroelectrics **264**, 133 (2001).
[18] G. Fischer, W. A. Adeagbo, A. Ernst, and W. Hergert (unpublished).
[19] C. Lee, Y. Park, and K. Kim, J. Korean Phys. Soc. **48**, 1570 (2006).
[20] S. Banerjee, M. Mandal, N. Gayathri, and M. Sardar, Appl. Phys. Lett. **91**, 182501 (2007).
[21] Q. Xu, L. Hartmann, H. Schmidt, H. Hochmuth, M. Lorenz, A. Setzer, P. Esquinazi, C. Meinecke, and M. Grundmann, Thin Solid Films **516**, 1160 (2008).
[22] N. Sanchez, S. Gallego, and M. C. Muñoz, Phys. Rev. Lett. **101**, 067206 (2008).
[23] S. Zhou *et al.*, J. Phys. D **41**, 105011 (2008).
[24] W. Anwand, H.-R. Kissener, and G. Brauer, Acta Physiol. Pol. **A88**, 7 (1995).
[25] *Positron Annihilation in Semiconductors*, edited by R. Krause-Rehberg and H. Leipner (Springer-Verlag Berlin Heidelberg, 1999).